

# The Effect of Phosphoric Acid Functionalization of Para-aramid Fiber on the Mechanical Property of Para-aramid Sheet

Zhaoqing Lu<sup>1,2</sup>, Yongsheng Zhao<sup>1,2</sup>, Zhiping Su<sup>1</sup>, Meiyun Zhang<sup>1</sup>, Bin Yang<sup>1</sup>

<sup>1</sup>College of Bioresources Chemical and Materials Engineering,  
Shaanxi University of Science & Technology, Xi'an, CHINA

<sup>2</sup>State Key Laboratory of Pulp and Paper Engineering, South China University of Technology, Guangzhou CHINA

Correspondence to:

Zhiping Su email: [18729586695@163.com](mailto:18729586695@163.com)

## ABSTRACT

The mechanical properties of para-aramid sheet (PAS) are mainly dependent on the interfacial property between para-aramid chopped fibers and fibrils. However, the chemical inertness and smooth surface of para-aramid chopped fiber lead to the poor interfacial adhesion between para-aramid chopped fibers and fibrils. In this study, para-aramid chopped fiber was treated by phosphoric acid (PA) solution with different concentration in order to prepare PAS with high mechanical strength. It was shown that PA-treatment can increase the surface roughness and improve the surface oxygen-containing active groups of para-aramid chopped fibers. In addition, there is a critical value of PA-concentration (20%). Proper PA-treatment gives rise to an increased tensile strength of PAS from 2.41 to 3.41 kN/m by an increment of 41.49%. However, excessive PA-treatment results in a dramatic reduction of tensile strength for para-aramid fibers and also for PAS possibly due to the structure destruction of para-aramid fiber. This work shows a simple but highly-efficient approach for improving the mechanical property of PAS via PA-treatment of para-aramid chopped fibers, and simultaneously elaborating the reinforcing effects for high-performance PAS especially through optimizing the interfacial property between para-aramid chopped fibers and fibrils.

## INTRODUCTION

Concerns over the energy security and high-speed orientation, urgent demands for advanced materials in potential applications including spacecraft, aircraft, automobile, rail transit, and marine fields have been hot topics over the past few years.

In comparison with conventional metal-based materials, the utilization of composite materials presents tremendous advantages in their lightweight structure and high strength. Aramid sheets, a kind of high-performance composite materials, have demonstrated various applications such as honeycomb structure materials [1], electrical isolation materials [2], and thermal isolation materials [3] used in aerospace, aviation, and automobile industries owing to their intrinsically appealing properties which include high strength, high modulus, high environmental resistance, low density, and outstanding thermal stability and dielectric ability [4,5]. However, it is worth noting that aramid sheets can be classified as two categories including meta-aramid sheet and para-aramid sheet according to the different chemical structure of aramid fibers. Compared with meta-aramid sheet, para-aramid sheet (PAS) owns many superior properties such as higher strength, more excellent thermal stability [6], and lower hygroscopicity [7]. Thus the foremost application of para-aramid sheet is used as honeycomb structure composite materials in some advanced fields, such as aviation and aerospace [8, 9].

PAS is entirely manufactured by combination of para-aramid polymers with two different morphologies including chopped fibers and fibrils [5, 10]. On one hand, chopped fibers play a role in reinforcing component in PAS due to their high stiffness and high modulus. On the other hand, the fibrils present a flexible morphology of non-granular, non-rigid, and microscopic film-like features and acts as the binder for chopped fibers, thus providing the final mechanical strength and

electrical properties for PAS. In general, interfacial adhesion of composite materials dominates its physical behaviors and related applications [11, 12]. Para-aramid chopped fiber possesses chemical inertness, smooth surface due to its highly crystalline structure and intermolecular interactions. The chemical inertness and smooth surface can hinder the chemical bonding and mechanical interlock with fibrils, resulting in a poor interfacial adhesion between para-aramid chopped fibers and fibrils and a limited application of PAS.

The interfacial adhesion between para-aramid fiber and polymer matrix can be improved by introducing polar components onto the surface and/or increasing the surface roughness of fiber [13,14]. Therefore, in order to achieve an activated surface for these fibers, many approaches have been conducted, for instance, plasma activation [15],  $\gamma$ -ray radiation [16, 17], ultrasound processing [18], surface coating [19], supercritical carbon dioxide treatment [20], grafting modification [21], chemical modification [22]. Although these methods can effectively increase para-aramid fiber/matrix interfacial adhesion strength, they also showed some apparent disadvantages. That is, plasma activation is not durable in surface modification with time [23], and most of these methods are only applicable to laboratory-scale researches but not to an industrial production. Recently, it is reported that phosphoric acid functionalization can effectively increase surface roughness and the content of oxygen-containing polar groups on the surface of para-aramid fiber, which can remarkably enhance the para-aramid fiber/polymer matrix interfacial strength [24–26]. However, previous studies tend to focus on the effect PA-treatment on the mechanical properties of para-aramid fiber/resin composite material. Only Sha et al [5] reported that PA-modification of meta-aramid fibers could dramatically improve the mechanical of meta-aramid sheet. Thereby there is an urgent need but it is still a great challenge to explore whether PA-modification is appropriate for para-aramid fibers for producing para-aramid sheet with more excellent mechanical property.

In this work, we focus on the effect PA-treatment on the structure and physical properties of para-aramid fiber by changing PA concentration and then to investigate the reinforcing mechanism of PA-functionalized para-aramid chopped fiber in

para-aramid sheet. The effect of PA-treatment on the surface characteristics of para-aramid chopped fiber, including surface morphology, surface roughness, surface chemical composition, and surface chemical structure were investigated by scanning electron microscopy (SEM), atomic force microscopy (AFM), X-ray photoelectron spectroscopy (XPS), and Fourier transform infrared spectroscopy (FT-IR), respectively. The mechanical property of para-aramid chopped fiber with PA-treatment was evaluated by monofilament tensile strength testing. In addition, the tensile strength testing was employed to determine the mechanical property of para-aramid sheet.

## **EXPERIMENTAL**

### **Materials**

Para-aramid chopped fibers (average length 5~6mm, average diameter 12 $\mu$ m) and fibrils used in this study were friendly supplied by Teijin Group in Japan. Phosphoric acid (AR) and acetone (AR) were obtained from Xi'an organic chemical plant. Epoxy resin HY 914 used to test monofilament tensile strength was purchased from Tianjin Haiyan Chemical Co., Ltd (China), which consists of two components: A (adhesion agent) and B (curing agent). Distilled water used in this work was prepared in laboratory.

### **Functionalization of Para-Aramid Chopped Fiber with Phosphoric Acid**

Before surface functionalization, the para-aramid chopped fibers were immersed in acetone solution with ultrasonic agitation for 4h to eliminate the surface contamination and then dried in oven at 105°C for 3h. Subsequently, the rinsed fibers were functionalized with 10, 20, 30, 40 wt% PA solution at 40°C for 2h, respectively [24]. Then the treated fibers were rinsed repeatedly with distilled water and dried at 105°C for 4h in a vacuum drying oven.

### **Surface Morphology and Topography and Observation**

The surface morphologies of PA-functionalized fibers and virgin fibers were observed by a FEI Q45+EDAX Octane Prime scanning electron microscopy (FEI and EDAX, America). To provide the conductivity for impinging electrons, prior to the SEM analysis the specimens were coated with gold for two min. The operation voltage and magnification were 7 kV and 5000, respectively.

A multimode SPI3800N/SPA400 AFM with a Nanoscope IIIa Controllor (Seiko, Japan) was employed to determine the surface topography and roughness of PA-functionalized samples and untreated samples. The AFM images with a scan area of  $1\mu\text{m}\times 1\mu\text{m}$  were obtained via a tapping mode.

### **Surface Chemical Composition and Chemical Structure Analysis**

To study the change of chemical composition on the surface of para-aramid fibers before and after PA-treatment, XPS analysis was performed on a Kratos ASMA 800 spectrometer (Kratos Analytical Ltd., UK), which was equipped with Al K $\alpha$  (1486.6eV) X-ray source, with the voltage of 15 kV, and the power of 250 W. During the test, the vacuum chamber pressure was maintained at the range of  $10^{-8}\sim 10^{-9}$  Torr. To investigate the surface chemical structure of original samples and PA-functionalized samples, fourier transform infrared spectroscopy (FT-IR) of samples were measured by a Bruker FT-IR spectrometer (Germany) with  $4\text{cm}^{-1}$  resolution in the mid infrared region ( $4000\text{-}400\text{cm}^{-1}$ ).

### **Monofilament Tensile Strength Measurement**

A para-aramid chopped fiber was randomly taken out from the prepared specimens, and then the two ends of fiber were fixed on a special plastic frame by the double-face adhesion tape. Subsequently, two droplets of epoxy resin which was mixed with adhesion agent and curing agent at the ratio 5:1 was dropped on the fiber surface, and the distance between the two droplets was controlled at 3mm with the deviation of 0.5mm. After the prepared samples were cured at  $105^{\circ}\text{C}$  for 24h, the monofilament tensile strength was measured via fiber mechanical properties testing instrument (JSF08, Shanghai Zhongchen digital technology equipment co., LTD, China) using a testing speed of 10mm/min at room temperature.

### **Preparation of Para-Aramid Sheet and its Mechanical Property Analysis**

PAS was prepared according to Tappi standard method (T 205 sp-95). A mixture of para-aramid chopped fibers and fibrils at the ratio 3:7 was disintegrated in water for 15000r by a Lorentzen & Wettre disperser (Sartorius, Germany) to obtain the uniform pulp suspension. Subsequently, the pulp suspension was diluted to 0.1% consistency. The target grammage of each PAS was  $45\text{g}/\text{m}^2$ . Herein, a

required amount of diluted pulp suspension was poured into a container and drained by an ERNST HAAGEBBS-3 sheet formation machine. The wet sample was pressed at 0.04MPa for 3min to remove excess water and followed by being dried at  $105^{\circ}\text{C}$  for 5min. Then to endow the produced sheet with excellent mechanical properties by enhancing the adhesive ability of fibrils, the dried sample was calendered by a double-roller calender at  $240^{\circ}\text{C}$ , 112 kN/m, and 1.5 m/min. The mechanical property of produced samples was determined by the measurement of tensile strength via a L&W SE-062 tensile tester with a load of 0.26 MPa according to Tappi standard method (T 494 om-88). The cross-section morphology of produced PAS was observed using a S4800 scanning electron microscopy (Hitachi). A thin Au layer was sputtered on the specimens before observing.

## **RESULTS AND DISCUSSION**

### **Effect of PA-Treatment on Surface Morphology of the Para-Aramid Fiber**

For comparison, surface morphology of para-aramid chopped fibers before and after PA-treatment is presented in *Figure 1*. *Figure 1(a)* shows an extremely clean and smooth surface of pristine para-aramid chopped fiber, which indicates a weak interfacial adhesion between para-aramid chopped fibers and fibrils. Compared with untreated fiber, the differences in the morphologies of PA-functionalized samples can be observed from *Figure 1(b-e)*. At 10% PA, the dotted pattern on fiber surface can be found (*Figure 1b*), which helps to improve the surface roughness of treated fibers. When 20% PA was used (*Figure 1c*), the surface of treated fiber appears more irregular and rougher. Meanwhile, it also shows a remarkable increase in the size of dotted pattern on the surface of treated fiber. When the PA concentration increases to 30% (*Figure 1d*), the surface presents an apparent damage involving the peeling of skin layer. This implies the intrinsic skin-core structure of para-aramid fiber is damaged by the strong corrosion from PA-treatment especially when the modification process is conducted at high PA concentration. However, when the PA concentration increases further to 40% (*Figure 1e*), the surface appears relatively smooth, meanwhile some grooves can be remarkably observed. These demonstrate that the skin layer of para-aramid chopped fiber could be thoroughly peeled off and the damage of the core layer could occur when excessive PA concentration was used.

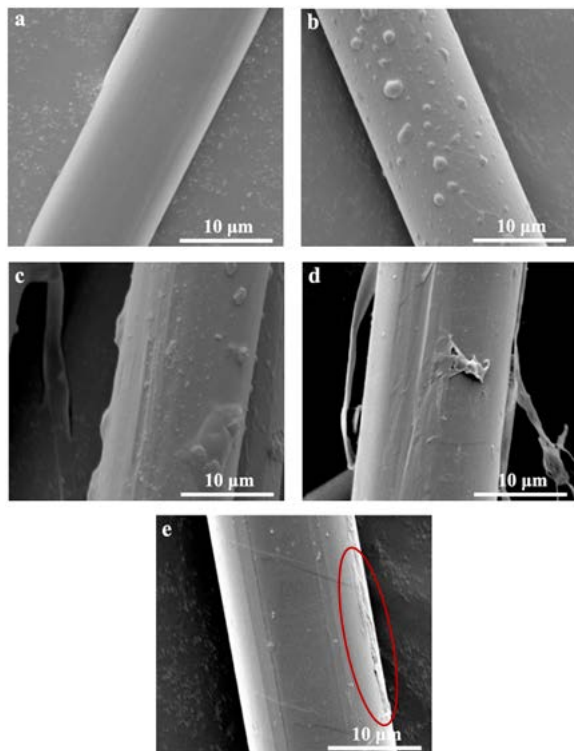


FIGURE 1. SEM images of (a) untreated, (b) 10% PA, (c) 20% PA, (d) 30% PA, and (e) 40% PA-functionalized para-aramid chopped fibers.

Table I summarized the surface roughness of untreated and treated para-aramid fibers, which are characterized in term of root mean square roughness ( $R_q$ ) and maximum height roughness ( $R_{max}$ ) [15]. The two-dimensional and three-dimensional microscopic topographies of para-aramid chopped fibers with or without PA-treatment are shown in Figure 2. The surface of original fiber is relatively smooth and inerratic with numerous repeated pleating stripes, which also verified from the low value of  $R_q$  and  $R_{max}$  (Table Ia). After 20% PA-treatment (Figure 2b), the surface topography of treated sample presents great difference. In addition, the surface roughness of treated fiber shows a drastic increase (Table Ib). For the sample treated by 40% PA (Figure 2c), the obvious decrease in the depth and quantity of grooves are observed along with deceased  $R_q$  and  $R_{max}$  (Table Ic). These can be ascribed to skin peeling of the treated fiber under strong erosion. The core layer of the fiber treated by 40% PA exposed, its surface is still highly rougher than untreated fiber. This phenomenon is related to

that the fibrils are more tightly connected and interlocked in the skin-line zone, but the core-like fibrils appear loose [27]. Thus damages were easily generated in core region, which led to a rougher surface of treated fiber.

TABLE I. Surface roughness of virgin and PA-functionalized para-aramid fibers.

Fiber sample	$R_q$ (nm)	$R_{max}$ (nm)
(a) Untreated	6.07	9.06
(b) Treated by 20% PA	19.08	52.41
(c) Treated by 40% PA	14	36.29

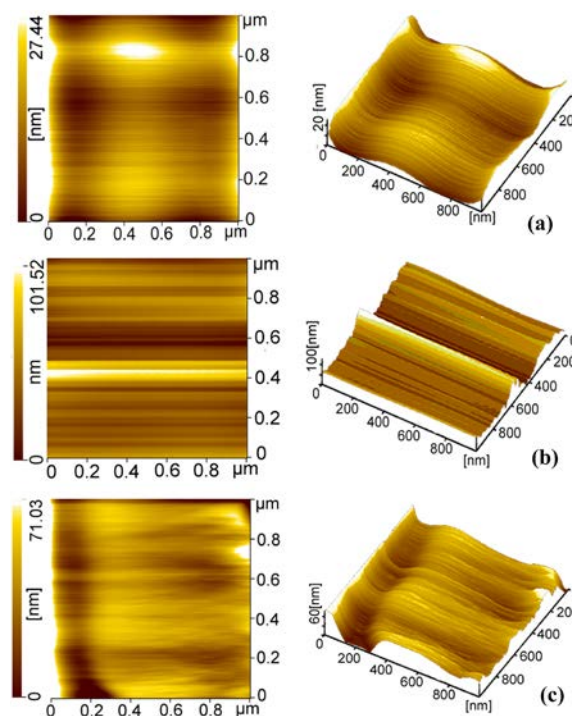


FIGURE 2. AFM images of (a) untreated, (b) 20% PA, and (c) 40% PA-functionalized para-aramid chopped fibers.

The results of AFM analysis, in consistency with SEM results (Figure 1), indicate that the surface roughness of para-aramid chopped fibers can be dramatically increased after PA-treatment. Moreover, the AFM analysis (Figure 2c) further demonstrates that when PA concentration over 40%, the skin-core structure of para-aramid chopped fiber was thoroughly destroyed and the core region are damaged.

### Effect of PA-Treatment on the Chemical Structure of Para-Aramid Fibers

The XPS analysis result of wide-scan spectrums was presented in *Figure 3*. It can be seen from the inset that the peak of oxygen element was strengthened after PA-treatment, which indicates some oxygen-containing active groups were successfully introduced on the surface of treated fibers. There must be chemical reaction as presented in *Figure 4*. The hydroxyl groups could be introduced in benzene ring by electrophilic substitution reaction (*Figure 4a*) [24]. In addition, a small quantity of polar carboxyl groups and amino groups could form due to the hydrolysis of some amide groups (*Figure 4b*) [24, 28]. The introduction of active oxygen-containing active groups on the surface of para-aramid chopped fibers by PA-treatment was also confirmed by FT-IR spectroscopy. As shown in *Figure 5*, upon functionalization with PA, the N-H stretching vibration peak at  $3302\text{cm}^{-1}$  increase obviously due to the increase of amino group by the hydrolysis of amide groups, and the N-H stretching vibration peak shift to lower wavenumbers that can be attributed to that hydrogen bonding was improved by the introduction of hydroxyl groups [5]. The double peak of amide II band containing C-N stretching vibration at  $1543\text{cm}^{-1}$  and N-H bending vibration at  $1511\text{cm}^{-1}$  disappears, indicating that the PA-treatment results in the formation of some carboxyl groups and amino groups.

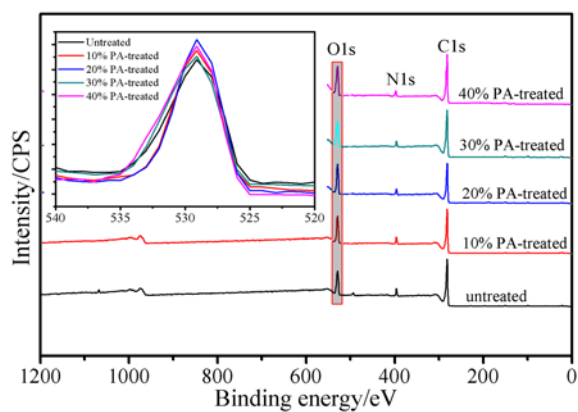


FIGURE 3. XPS wide scan spectrums of (a) untreated, (b) 10% PA, (c) 20% PA, (d) 30% PA, and (e) 40% PA-functionalized para-aramid chopped fibers. The inset is the enlarged figure of the peak of oxygen element.

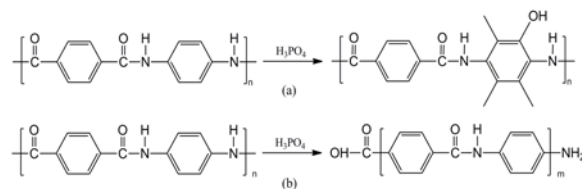


FIGURE 4. The scheme of electrophilic substitution reaction (a) and hydrolysis reaction process (b) on PA-functionalized para-aramid chopped fibers surface [24].

To further quantitatively analyze the change of surface elements composition after PA-treatment, the content of C, O, and N elements were determined by wide scan spectrums with the aid of Casa XPS software. *Figure 6* shows that the content of O element and O/C ratio were increased after PA-treatment. However, when PA concentration is over 20%, the content of O element and O/C ratio decreased. These reflects that the hydrolysis reaction tend to occur at the skin layer of para-aramid fibers during PA-treatment. As the skin layer of para-aramid fibers was peeled off when PA concentration is over 20%, a decrease in O element content and O/C ratio occurs. Herein, it reveals that an appropriate concentration (20%) exists for PA-treatment of the fibers.

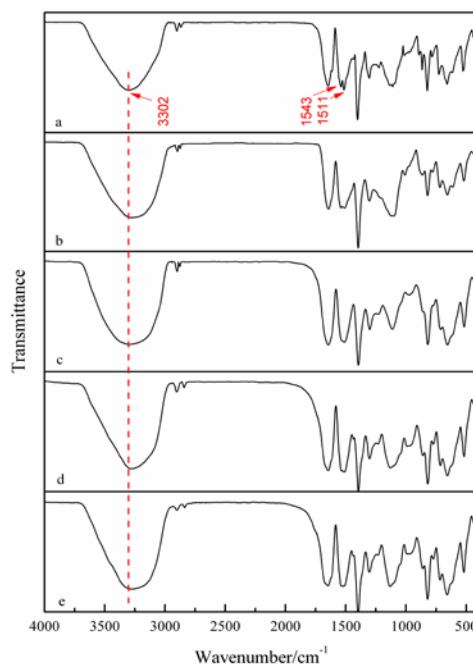


FIGURE 5. FT-IR spectra of (a) untreated, (b) 10% PA, (c) 20% PA, (d) 30% PA, and (e) 40% PA-functionalized para-aramid chopped fibers.

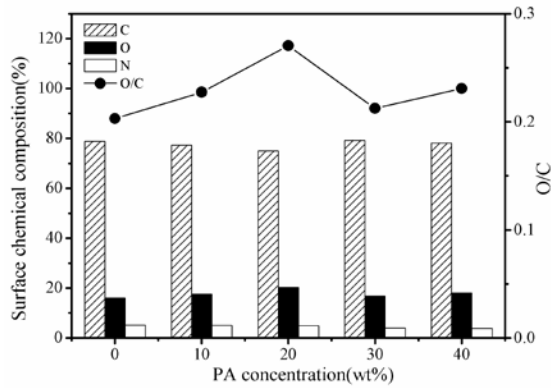


FIGURE 6. C, O, and N element content and O/C ratio on virgin and PA-functionalized para-aramid chopped fibers surface.

### **Effect of PA-Treatment on Mechanical Property of Para-Aramid Fibers**

Figure 7 shows the representative load-displacement curves of pristine and PA-functionalized para-aramid chopped fibers, which is consistent with the morphological data. It can be found that with the increase in PA concentration, the Young's modulus greatly increases but the toughness decreases for para-aramid fibers. This is mainly due to the stronger etching effect on the skin layer and thus increasing the overall crystallinity. In addition, the load-displacement curves also revealed that the maximum fracture load of para-aramid chopped fibers decreased significantly once PA concentration is over 20%. Figure 8 shows the relationship between monofilament tensile strength of para-aramid chopped fiber and PA concentration. It can be found that the monofilament tensile strength decreased obviously as the PA concentration increased over 20%. Below 20wt% PA-concentration, the tensile strength can be improved to a high value of 3.41 kN/m with an increment of 41.49%.

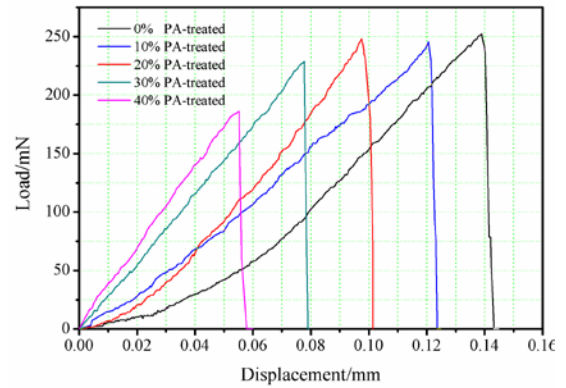


FIGURE 7. The load-displacement curves of untreated and PA-functionalized para-aramid chopped fibers.

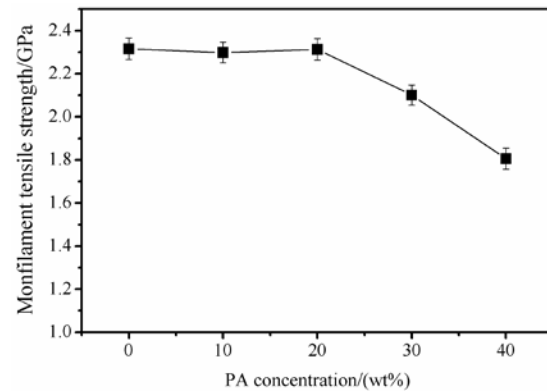


FIGURE 8. The effect of PA concentration on monofilament tensile strength of para-aramid chopped fiber.

### **Effect of PA-treatment on the mechanical strength of PAS**

Figure 9 shows the effect of PA concentration on the tensile strength of PAS. It reveals that the functionalization of para-aramid chopped fibers by PA can improve the tensile strength of PAS. In addition, the PAS which was made from para-aramid chopped fibers functionalized by 20% PA solution presents the highest tensile strength.

These results indicate that the changes of surface characteristics of para-aramid chopped fiber by PA-treatment can significantly optimize the interface properties between para-aramid chopped fibers and fibrils, thus leading to the improvement of tensile strength. The dramatic improvement in tensile strength of PAS can be supported by the SEM results of cross-section morphology of PAS. As *Figure 10a* shows that chopped fibers and fibrils present a poor mechanical interlocking and interfacial adhesion at interface region due to the excessively smooth surface of untreated chopped fibers, limiting the reinforcement and leading to a poor tensile strength of PAS. However, the interfacial properties between chopped fibers and fibrils were improved after PA-treatment as can be seen in *Figure 10b*. This is mainly caused by the increase in surface oxygen-containing active groups and surface roughness, which can induce that fibrils tightly adhere to the surface of chopped fibers and fibrils embedded in the grooves on the surface of PA-functionalized chopped fibers.

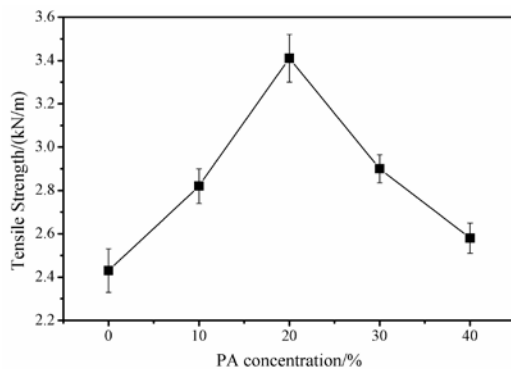


FIGURE 9. The effect of PA concentration on tensile strength of PAS.

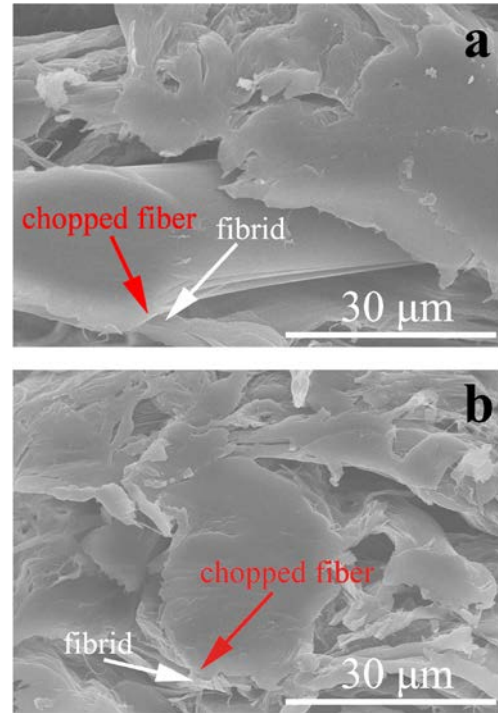


FIGURE 10. SEM images of the cross-section of para-aramid sheet containing (a) untreated chopped fibers, (b) 20% PA-functionalized para-aramid chopped fibers.

## CONCLUSION

In summary, the effect of PA-treatment especially with different concentration on mechanical property of para-aramid chopped fiber and the resultant PAS sheet was investigated. It was found that PA-treatment can improve the surface roughness and surface chemical activity of para-aramid chopped fiber, which is helpful to further enhance mechanical strength for PAS through adding PA-functionalized para-aramid chopped fiber. Firstly, the monofilament tensile strength of para-aramid chopped fiber was nearly constant until the functionalization by 20% PA solution, while it obviously decreased as PA concentration is over 20%. Compared to the PAS prepared with untreated para-aramid chopped fiber, the tensile strength of para-aramid sheet containing PA-treated fibers can be improved from 2.41 to 3.41 kN/m by an increment of 41.49%. The remarkable enhancement of tensile strength is mainly attributed to the fact that PA-functionalization can greatly optimize the properties of the interfacial properties between chopped fibers and fibrils by increasing mechanical interlock effect and interfacial adhesion.

## ACKNOWLEDGEMENT

The authors would like to acknowledge the financial support from State Key Laboratory of Pulp and Paper Engineering (201727), Shaanxi Province as a Whole the Innovation Project of Science and Technology Plan Projects (2016KTCQ01-87), Key Laboratory Project Funded by Education Department of Shaanxi Provincial Government (12JS018), and State Key Laboratory of Fiber Materials Modification (LK1601).

## REFERENCES

- [1] Liu, L., et al, The flatwise compressive properties of Nomex honeycomb core with debonding imperfections in the double cell wall, *Composites Part B: Engineering*, 76, 2015, 122–132.
- [2] Tuncer, E., et al, Electrical properties of commercial sheet insulation materials for cryogenic applications, *Annual Report - Conference on Electrical Insulation and Dielectric Phenomena*, 2008, 301–304.
- [3] Yang B., et al, A ductile and highly fibrillating PPTA-pulp and its reinforcement and filling effects of PPTA-pulp on properties of paper-based materials, *Journal of Applied Polymer Science*, 133, 13, 2016, 1–6.
- [4] Lu Z., et al, Characteristics of PPTA Chipped Fiber/Fibrid and their Properties for Sheet Making, *Journal of Engineered Fibers and Fabrics*, 11, 1, 2016, 1–8.
- [5] Sha L., Zhao, H., Effect of Surface Modification Process Conditions on Properties of Aramid Paper, *Polymer (Korea)*, 37, 2, 2013, 196–203.
- [6] Brown J., Ennis B., Thermal Analysis of Nomex(R) and Kevlar(R) Fibers, *Textile Research Journal*, 47, 1, 1977, 62–66.
- [7] Jiang M., Structures and Properties Comparison of Meta- aramid and Para-aramid Fibrid and Their Paper-based Insulation Materials, *Insulating Materials*, 50, 1, 2017, 17–22.
- [8] Lu Z., et al, Toward high-performance poly (para-phenylene terephthalamide) (PPTA)-based composite paper via hot-pressing: the key role of partial fibrillation and surface activation, *RSC Advances*, 7, 12, 2017, 7293–7302.
- [9] Lu Z., et al, Argon low-temperature plasma modification of chopped aramid fiber and its effect on paper performance of aramid sheets, *Journal of Applied Polymer Science*, 134, 34, 2017, 45215–45224.
- [10] Zhao, H., et al, Influence of Fiber Characteristics and Manufacturing Process on the Structure and Properties of Aramid Paper, *Polymer-Plastics Technology and Engineering*, 51, 2, 2012, 134–139.
- [11] Day, R.J., Hewson, K.D., Lovell, P.A., Surface modification and its effect on the interfacial properties of model aramid-fibre/epoxy composites, *Composites Science and Technology*, 62, 2, 2002, 153–166.
- [12] Ge, X., et al, Effects of silane coupling agents on the properties of bentonite/nitrile butadiene rubber nanocomposites synthesized by a novel green method, *Applied Clay Science*, 118, 2015, 265–275.
- [13] Jang, J., Yang, H., The effect of surface treatment on the performance improvement of carbon fiber/polybenzoxazine composites, *Journal of Materials Science*, 35, 9, 2000, 2297–2303.
- [14] Jiang, D., et al, Reinforced unsaturated polyester composites by chemically grafting amino-POSS onto carbon fibers with active double spiral, *Composites Science and Technology*, 100, 2014, 158–165.
- [15] Jia, C., et al, Surface wettability of atmospheric dielectric barrier discharge processed Armos fibers, *Applied Surface Science*, 258, 1, 2011, 388–393.
- [16] Xing, L., et al, Enhanced interfacial properties of domestic aramid fiber-12 via high energy gamma ray irradiation, *Composites Part B Engineering*, 69, 2015, 50–57.
- [17] Zhang, Y., et al, The modification of Kevlar fibers in coupling agents by  $\gamma$ -ray co-irradiation, *Fibers and Polymers*, 12, 8, 2011, 1014–1020.
- [18] Liu, L., et al, Ultrasonic treatment of aramid fiber surface and its effect on the interface of aramid/epoxy composites, *Applied Surface Science*, 254, 9, 2008, 2594–2599.
- [19] Chen, J., et al, Surface modification and characterization of aramid fibers with hybrid coating, *Applied Surface Science*, 321, 2014, 103–108.

- [20] Kong, H., et al, Surface modification of poly (p-phenylene terephthalamide) fibers with HDI assisted by supercritical carbon dioxide, *RSC Advances*, 5, 72, 2015, 58916–58920.
- [21] Sa, R., et al, Improved adhesion properties of poly-p-phenyleneterephthamide fibers with a rubber matrix via UV-initiated grafting modification, *RSC Advances*, 5, 114, 2015, 94351–94360.
- [22] Liu, T.M., Zheng, Y.S., Hu, J., Surface modification of aramid fibers with novel chemical approach, *Polymer Bulletin*, 66, 2, 2011, 259–275.
- [23] Sanchis, M.R., et al, Characterization of the surface changes and the aging effects of low-pressure nitrogen plasma treatment in a polyurethane film, *Polymer Testing*, 27, 1, 2008, 75–83.
- [24] Li, G., et al, Interface correlation and toughness matching of phosphoric acid functionalized Kevlar fiber and epoxy matrix for filament winding composites, *Composites Science and Technology*, 68, 15-16, 2008, 3208–3214.
- [25] Li, J., Xia, Y.C., Interfacial characteristics of an epoxy composite reinforced with phosphoric acid-functionalized Kevlar fibers, *Mechanical of Composite Materials*, 46, 2, 2010, 211–214.
- [26] Zhao J., Effect of surface treatment on the structure and properties of para-aramid fibers by phosphoric acid, *Fibers and Polymers*, 14, 1, 2013, 59–64.
- [27] Rebouillat, S., Peng, J.C., Donnet, J.-B., Surface structure of Kevlar® fiber studied by atomic force microscopy and inverse gas chromatography, *Polymer*, 40, 1999, 7341–7350.
- [28] Mosquera, M.E.G., et al, Thermal Transformations of Kevlar Aramid Fibers during Pyrolysis: Infrared and Thermal Analysis Studies, *Chemistry of Materials*, 6, 11, 1994, 1918–1924.

#### AUTHORS' ADDRESSES

**Zhaoqing Lu**  
**Yongsheng Zhao**  
**Zhiping Su**  
**Meiyun Zhang**  
**Bin Yang**

College of Bioresources Chemical and Materials  
 Engineering  
 Shaanxi University of Science & Technology Xi'an  
 710021  
 CHINA

**Zhaoqing Lu**  
**Yongsheng Zhao**  
 State Key Laboratory of Pulp and Paper  
 Engineering  
 South China University of Technology  
 Guangzhou, 510640  
 CHINA